

Journal of Maps



ISSN: (Print) 1744-5647 (Online) Journal homepage: https://www.tandfonline.com/loi/tjom20

Glacial geomorphology of the Strait of Magellan ice lobe, southernmost Patagonia, South America

Rodrigo L. Soteres, Carly Peltier, Michael R. Kaplan & Esteban A. Sagredo

To cite this article: Rodrigo L. Soteres, Carly Peltier, Michael R. Kaplan & Esteban A. Sagredo (2020) Glacial geomorphology of the Strait of Magellan ice lobe, southernmost Patagonia, South America, Journal of Maps, 16:2, 299-312, DOI: 10.1080/17445647.2020.1736197

To link to this article: https://doi.org/10.1080/17445647.2020.1736197







Science

OPEN ACCESS



Glacial geomorphology of the Strait of Magellan ice lobe, southernmost Patagonia, South America

Rodrigo L. Soteres ⁽¹⁾ a, Carly Peltier^{c,d}, Michael R. Kaplan^c and Esteban A. Sagredo^{a,b,e}

^aInstituto de Geografía, Pontificia Universidad Católica de Chile, Santiago, Chile; ^bMillennium Nucleus Paleoclimate, Millennium Science Initiative, Santiago, Chile; ^cLamont-Doherty Earth Observatory of Columbia University, Palisades, New York, USA; ^dDepartment of Earth and Environmental Sciences, Columbia University, New York, USA; ^eEstación Patagonia de Investigaciones Interdisciplinarias UC, Pontificia Universidad Católica de Chile, Santiago, Chile

ABSTRACT

We present a geomorphic map of the landforms created by the Patagonian Ice Sheet during the local Last Glacial Maximum and perhaps prior glaciations in southernmost Patagonia. Building on prior work, the new mapping focuses in unprecedented detail on the right lateral and frontal landforms formed by the Strait of Magellan ice lobe. We produced the map using aerial orthophotography, Sentinel-2 and SPOT satellite imagery, ALOS PALSAR digital elevation model and fieldwork to ground-truth preliminary interpretations. We delineate at least five glacial events defined by a sequence of moraine drifts and associated glaciofluvial features. In contrast to previous studies, we propose the Magellan ice lobe extended ~65 km farther, to the Primera Angostura peninsula, during the local Last Glacial Maximum. Our study provides a new context to establish a precise glacial chronology of the Magellan ice lobe during the last glacial cycle in the middle-high latitudes of the Southern Hemisphere.

ARTICLE HISTORY

Received 14 August 2019 Revised 13 January 2020 Accepted 20 February 2020

KEYWORDS

Glacial geomorphology; last glacial maximum; Strait of Magellan; surface exposure dating; Patagonia

1. Introduction

Detailed mapping of ice marginal and subglacial landforms, especially moraines, is widely used to elucidate past ice-sheet fluctuations and dynamics. In turn, deciphering the timing of former glacial pulses contributes to the assessment of the mechanisms behind both past climate (Mackintosh, Anderson, & Pierrehumbert, 2017) and nonclimate changes (e.g. calving dynamics).

The Strait of Magellan area in southern Patagonia is a key site for paleoclimate research because it holds some of the oldest and best-preserved glacial features in the southern hemisphere, which reflects the presence of extensive glaciers since the Late Miocene (e.g. Clague et al., 2020; Mercer, 1976; Rabassa & Coronato, 2009). This exceptional record presents the potential to decipher past glacial activity in the southern hemisphere mid-latitudes and thus offers an opportunity to test the synchronicity of past glacial events at both hemispheric and global scale (Denton et al. 1999b; Lowell et al., 1995; Sugden et al., 2005).

In past decades, significant efforts have been made to unravel the glacial history of southern South America by dating glacial landforms. Most studies have focused on the glacial limits of the local Last Glacial Maximum (lLGM; ~33–18 ka; e.g. Denton et al.,

1999a; Douglass, Singer, Kaplan, Mickelson, & Caffee, 2006; Hein et al., 2010; Kaplan, Ackert, Singer, Douglass, & Kurz, 2004; McCulloch, Fogwill, Sugden, Bentley, & Kubik, 2005), leaving older glacial records relatively unstudied, with exceptions (e.g. Clague et al., 2020; Hein et al., 2009, 2017; Kaplan, Douglass, Singer, Ackert, & Caffee, 2005; Singer, Ackert, & Guillou, 2004).

Recent research on former glaciations near the Strait of Magellan area (Darvill, Stokes, Bentley, & Lovell, 2014; Darvill, Bentley, Stokes, Hein, & Rodés, 2015) focused mainly on the glacial landforms to the south linked to the Bahía Inútil-San Sebastián ice lobe. Here we extend finer detail mapping to the area covered specifically by the Magellan ice lobe. Our motivation is to map and describe previously inferred lLGM and pre-lLGM glacial drifts which run along northern Strait of Magellan and westernmost Tierra del Fuego (Benn & Clapperton, 2000; Meglioli, 1992). Additionally, we also reinterpret ¹⁰Be ages in Kaplan et al. (2007), particularly in light of the recent nearby work of Darvill, Bentley, Stokes, Hein, and Rodés (2015), to assess the extent and relations between pre-lLGM glacial drifts; this provides a new spatial context for regional glacial chronology.

CONTACT Rodrigo L. Soteres a risoteres@uc.cl Instituto de Geografía, Pontificia Universidad Católica de Chile, Avda. Vicuña Mackenna 4860, Macul, Santiago, Chile

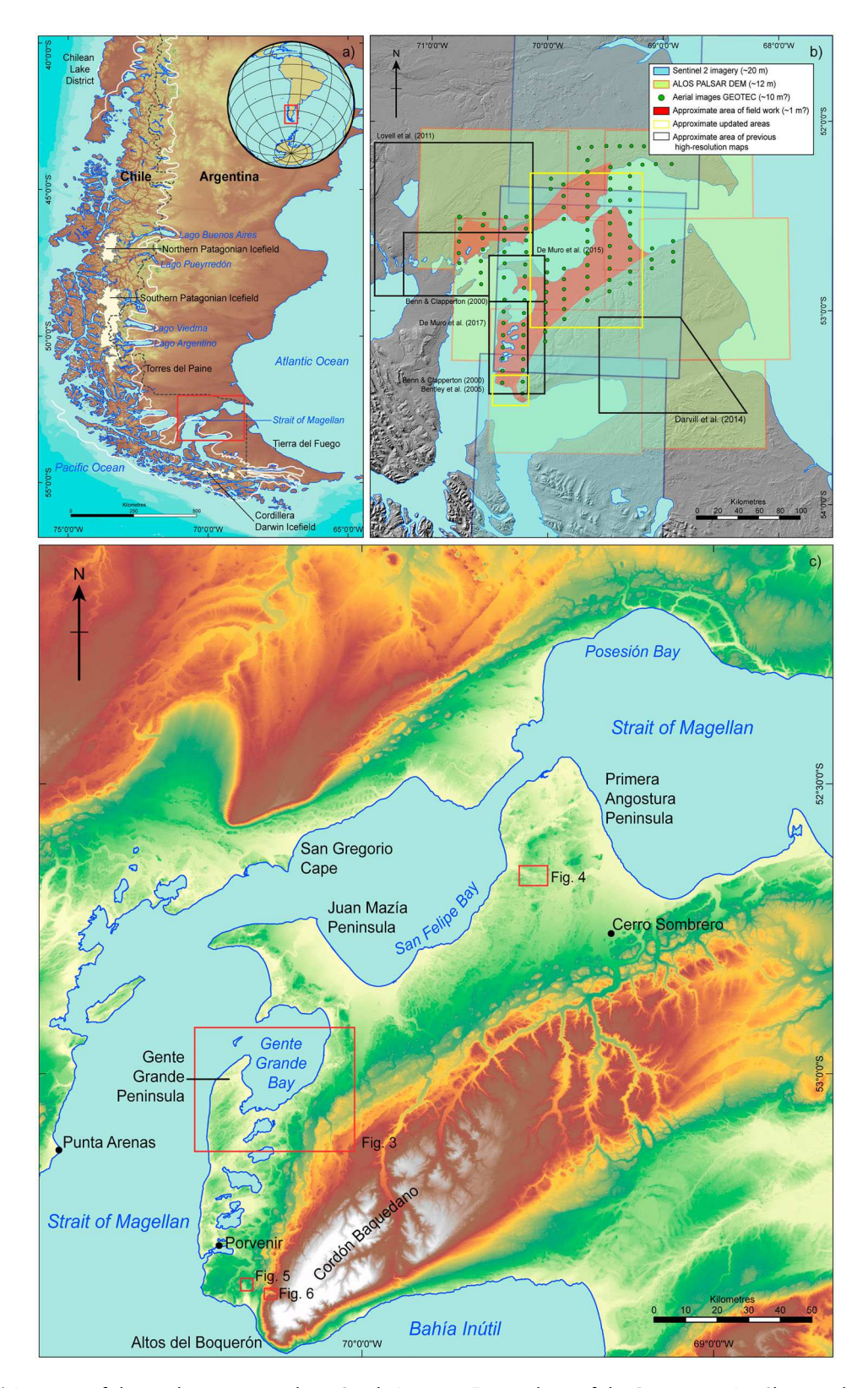


Figure 1. (a) Location of the study area in southern South America. Former limit of the Patagonian Ice Sheet is shown as a solid white line (Caldenius, 1932). Present Patagonian Ice Fields are depicted in white. (b) Overview of the Strait of Magellan region showing areas covered by previously published high-resolution geomorphic maps (black boxes) with highlighting updated areas (yellow boxes). Also shown the spatial coverage of used aerial (green dots: centroids of GEOTEC images) and satellite imagery (light blue boxes: Sentinel 2; light green boxes: ALOS PALSAR digital elevation model). (c) Digital elevation model of the Strait of Magellan region showing the main sites of the study area. Locations of the figures are delineated as red boxes.

2. Setting

The study area spans from 52°00′ to 54°00′S in South America (Figure 1(a)). The northern Strait of Magellan and westernmost Tierra del Fuego are dominated by a

wide variety of glacial landforms and major Strait of Magellan oceanic waterways, which run NE-SW between Primera Angostura and Juan Mazía Peninsula, and N-S from the latter to Bahía Inútil (Figure 1(b)).

The surface geology consists of marine and continental Tertiary sedimentary sequences and Quaternary glacial, glaciolacustrine and glaciofluvial deposits (SER-NAGEOMIN, 2003).

Regional climate is largely controlled by the southern westerly winds (Garreaud, Lopez, Minvielle, & Rojas, 2013), that are profoundly influenced by the austral Andes, resulting in a strong precipitation gradient between western and eastern Patagonia. To a lesser extent, easterly-derived moisture also impact the study area (Garreaud, Vuille, Compagnucci, & Marengo, 2009). The town of Punta Arenas $(53^{\circ}18'S - 70^{\circ}$ 22'W) has a mean annual temperature of ~6.5°C and a total precipitation of ~500 mm (Butorovic, 2016). This semiarid climate is partly responsible for the excellent preservation of the glacial landforms at this site and more generally on east flank of the Andes in Patagonia.

3. Previous Work

The Strait of Magellan region was occupied during successive glaciations by outlet glacial lobes flowing from the Andes towards the Atlantic Ocean (Mercer, 1976; Singer et al., 2004). From north to south, the major ice lobes are Río Gallegos, Skyring, Otway, Magellan and Bahía Inútil-San Sebastián (Figure 2(a) and Table 1).

Early maps of the former ice lobes covering the region were presented by Nordenskjöld (1899) and Caldenius (1932), who identified the major moraine complexes across Patagonia. However, the first relatively detailed map of the Strait of Magellan area was presented by Meglioli (1992), although he described 'surface units' rather than glacial landforms assemblages.

Subsequently, Clapperton, Sugden, Kaufman, and McCulloch (1995) depicted on a broad scale the glacial drifts formed by the Magellan ice lobe (Figure 2(b)). They labeled these features, from the outermost (oldest) to the innermost (youngest) as the A, B, C, D and E limits. Additionally, they and others compiled precise geomorphic maps of punctual areas assumed to have been ice-covered during the lLGM (i.e. B to D limits; Benn & Clapperton, 2000; Bentley, Sugden, Hulton, & McCulloch, 2005). Unlike inner limits, which are clearly identified, the extent of the A limit was only depicted to the south of Juan Mazía Peninsula (Figure 2(b)). From that location, authors inferred that the limit heads north towards the ocean, reappearing on the mainland on the north side of the Strait of Magellan (Figure 2(b)). This conceptual model of the A-D limits was a basis to interpret the chronology of past glacial pulses in the region by McCulloch et al. (2005) and Kaplan et al. (2007, 2008). However, the lack of the detailed mapping of the A limit, which included inferred pre-lLGM landforms (e.g. Bentley et al., 2005; Clapperton et al., 1995), raises uncertainty in our understanding of the regional glacial

Recently, Lovell, Stokes, and Bentley (2011) and Darvill et al. (2014) produced extensive geomorphic maps of the region focusing on the areas covered by the Seno Skyring, Seno Otway and Bahía Inútil-San Sebastián ice lobes. The most recent geomorphic maps focus on coastal landforms within discreet areas of the Strait of Magellan (DeMuro, Brambati, Tecchiato, Porta, & Ibba, 2017; DeMuro, Di Grande, Brambati, & Ibba, 2015).

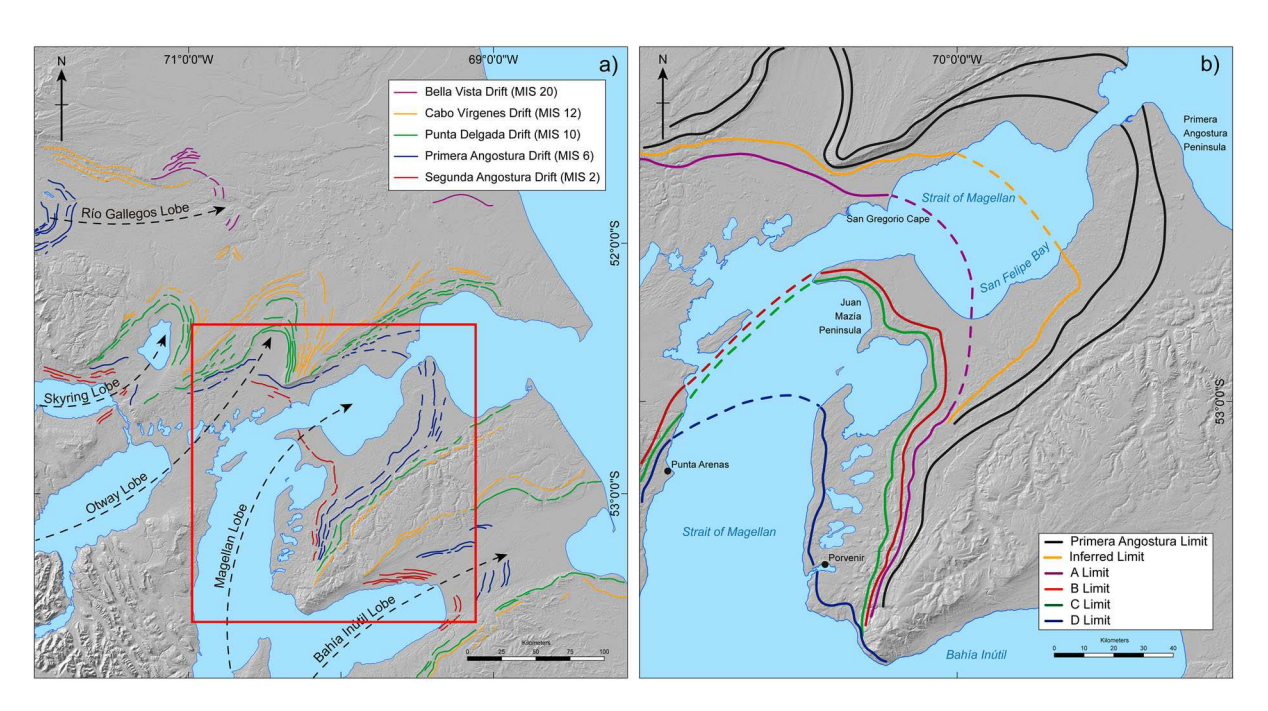


Figure 2. (a) Major glacial limits in the Strait of Magellan region. The limits extent is based on Coronato, Ercolano, Corbella, and Tiberi (2013). Map legend refers limits as termed by Meglioli (1992) and marine isotopes stages of the drifts according to Rabassa and Coronato (2009). (b) Major glacial limits in the Strait of Magellan and westernmost Tierra del Fuego as depicted by Benn and Clapperton (2000). Primera Angostura drift extent is based on Meglioli (1992)

Pioneering work to date glacial limits in southern Patagonia was conducted by Caldenius (1932). Based on varve counting, he concluded that the major glacial limits in Patagonia were formed during the last glaciation. However, radiometric chronological techniques have outlined a more complex Patagonian glacial history, encompassing multiple glacial cycles (e.g. Clapperton et al., 1995; Darvill et al., 2015; Kaplan et al., 2007, 2008; McCulloch et al., 2005; Meglioli, 1992; Mercer, 1976; Singer et al., 2004).

The oldest glacial drift in the region is the Bella Vista drift (Figure 2(a)) and corresponds to the Greatest Patagonian Glaciation (Mercer, 1976). 40Ar/39Ar and K/Ar dating constraints the age of the latter at ~1.1 Ma (Meglioli, 1992; Mercer, 1976; Singer et al., 2004).

The inner Magellan ice lobe drifts are 'nested' within the boundary of Mercer's (1976) Greatest Patagonian Glaciation. The first inner moraine complex, named Cabo Vírgenes drift (Figure 2(a)), was assigned to MIS 12 based on minimum 40 Ar/ 39 Ar ages of 0.45 ± 0.1 and 0.36 ± 0.04 Myr (Meglioli, 1992; Rabassa & Coronato, 2009). Recent studies to the south, based on cosmogenic exposure of boulders of the Río Cullen drift, the correlative unit for the Bahía Inútil ice lobe (Figure 2(a); Table 1), have yielded significantly younger ages ranging from 13.2 ± 7.0 to 54.0 ± 5.5 ka (Evenson, Burkhart, Gosse, & Baker, 2009; Kaplan et al., 2007). Either the mapped Cabo Vírgenes drift for the Bahía Inútil and Strait of Magellan ice lobes are not correlative (Meglioli, 1992), or the innermost parts of the Cabo Vírgenes drift of the Bahía Inútil were deposited during MIS 3 and/or 4 (Darvill et al., 2015).

Inbound, the Punta Delgada drift (Figure 2(a)) was first considered MIS 10 in age based on inferred correlation to a uranium-series dated marine terrace on eastern Tierra del Fuego (Bujalesky, Coronato, & Isla, 2001; Rabassa & Coronato, 2009). However, a suite of cosmogenic exposure ages on Punta Delgada drift boulders have provided minimum-limiting ages ranging between \sim 21.0 \pm 1.0 and \sim 174.0 \pm 4.0 ka (Kaplan et al., 2007). Moreover, Darvill et al. (2015) carried out cosmogenic dating through depth profiles in outwash plains obtaining an age of ~30.1 ka for the correlative glacial limit of the Punta Delgada drift in Bahía Inútil, leading the authors to conclude a much younger age (late MIS 3).

The inboard drift was named Primera Angostura. Initially, it was indirectly dated according to its morphostratigraphic position as MIS 6 (Figure 2(a); Meglioli, 1992; Rabassa & Coronato, 2009). However, the age of A limit (Figure 2(b)) identified by Clapperton et al. (1995), which occupies a similar position to Primera Angostura drift, was estimated to be between 90 and 130 ka, corresponding to MIS 5, based on maximum limiting amino acid ages obtained from mollusc shells embedded in till deposits (Clapperton et al., 1995; McCulloch et al., 2005). Although the ages of Primera Angostura and A limit drifts are poorly constrained, it has been widely accepted that both reflect pre-lLGM glacial events, that most likely occurred during MIS 6 (Coronato, Meglioli, & Rabassa, 2004; Meglioli, 1992; Rabassa & Coronato, 2009). More recently, Kaplan et al. (2007) obtained direct cosmogenic ages for the Primera Angostura drift, which range originally between $\sim 21.2 \pm 1.6$ and $\sim 31.6 \pm$ 3.4 ka, but were interpreted as minimum-limiting ages, given the conceptual model proposed at the time. However, these ages, collectively with those from Darvill et al. (2015) on outwash associated to the Punta Delgada drift (i.e. ~30.1 ka) suggest that the Primera Angostura drift/ A limit was deposited during the early MIS 2 or late MIS 3 (Darvill, Stokes, Bentley, Evans, & Lovell, 2016).

The chronology of the inner glacial drifts (i.e. B, C and D; Figure 2(a)) was first established through radiocarbon and amino acid techniques (Clapperton et al., 1995; Porter, 1990) and afterwards revised and complemented with tephrochronology, cosmogenic nuclide ages and optically simulated luminescence (Blomdin et al., 2012; Kaplan et al., 2008; McCulloch et al., 2005). The set of available surface exposure ages for B and C limits (i.e. Juan Mazía drift) indicate that they were deposited between \sim 25.6 \pm 1.5 and \sim 23.5 \pm 0.8 ka and 19.9 ± 1.2 and 15.7 ± 2.6 ka, respectively. Based on these ages, most authors have considered these drifts as the outermost geomorphic limit of the lLGM (i.e. MIS 2 glaciation; Kaplan et al., 2008; McCulloch et al., 2005).

Finally, ¹⁴C and ¹⁰Be ages indicate that the Magellan ice lobe retreated from the D limit (Figure 2(b)) by ~17 ka (Hall, Porter, Denton, Lowell, & Bromley, 2013). This glacial drift has been inferred to be the last major lLGM position in the Strait of Magellan area (Kaplan et al., 2008; McCulloch et al., 2005).

Table 1. Stratigraphic names of the Magellan ice lobe drift sequence identified by Meglioli (1992) and its correlatives units from Bahía Inútil-San Sebastián and Río Gallegos ice lobes (Rabassa et al., 2000).

		· · · · · · · · · · · · · · · · · · ·	
Age	Magellan ice lobe	Bahía Inútil-San Sebastián ice lobe	Río Gallegos ice lobe
Older	Sierra de los Frailes Drift	Pampa de Beta Drift	Bella Vista Drift
†	Cabo Vírgenes Drift	Rio Cullen Drift	Glencross Drift
	Punta Delgada Drift	Sierras de San Sebastián Drift	Not recognized
+	Primera Angostura Drift/A limit	Lagunas Secas Drift	Rio Turbio Drift
Younger	Segunda Angostura Drift/B limit	Bahía Inútil Drift	Seno Almirante Montt Drift



4. Map Production

Our geomorphic map has been built upon previous maps of the region (Benn & Clapperton, 2000; Bentley et al., 2005; Clapperton et al., 1995; Darvill et al., 2014; Glasser & Jansson, 2008; Glasser, Jansson, Harrison, & Kleman, 2008; McCulloch et al., 2005; Meglioli, 1992) by combining remote sensing analysis and exhaustive fieldwork (Chandler et al., 2018).

The main sources were GEOTEC orthophotos (1/ 70000) produced by the Chilean Servicio Aerofotogramétrico de la Fuerza Aérea, Google Earth (2016 Cnes/ SPOT, ~15 m spatial resolution), SENTINEL-2 (~20 m spatial resolution) and ESRI Imagery (2017, TerraColor, ~15 m spatial resolution and SPOT, ~2.5 m spatial resolution). Advance Land Observation Satellite (ALOS PALSAR, ~12 m spatial resolution) digital elevation models were examined to identify minor glacial features when interpretation using imagery was challenging.

5. Results

5.1. Glacial geomorphology

We classified landforms assemblages into the following categories: ice-marginal, subglacial, glaciofluvial and other features, to allow comparison with previous interpretations of the regional geomorphic record (Table 2).

5.2. Ice-marginal features

5.2.1. Moraine drift

Moraine drifts are the major glacial landforms in the region and form a nested sequence of former glacier limits (Figure 3). Recently, Darvill et al. (2014) defined these units as kettle-kame topography. While moraine drifts can be imprinted with kettle-kame topography, because these landforms correspond to the lateral and frontal margins of the Magellan ice lobe, we prefer to refer them as moraine drifts.

Moraine drifts consists of linear or arcuate positive-relief features that extend for several kilometres (>100 km) along the flanks of the Strait of Magellan. These complexes can reach ~4 km wide and they rise over the surrounding landscape by tens of meters. The tops of the moraine drifts present sharp irregular terrain with scattered boulders. Grading from the moraine drifts, we found extensive outwash plains. Meltwater channels frequently dissect moraine drifts.

We have identified at least five moraine drifts in westernmost Tierra del Fuego, located at elevations that range from ~300 to ~25 m.a.s.l., from the outermost to the innermost. According to their morphostratigraphic position, preservation and 10Be ages in Kaplan et al. (2007), we have classified them as ILGM moraine drifts (red on map) and pre-lLGM (green on map).

5.2.2. Moraine ridges

Groups of minor moraine ridges (Figure 3(b)) are frequent inboard of major moraine drifts, where they appear superimposed on drumlinized and moraine terrain in the north inland of the Strait of Magellan and westernmost Tierra del Fuego. These features have been previously interpreted as recessional moraines (Clapperton, 1989). The ridges exhibit sharp crestlines and linear to arcuate planform. They can have lengths of tens of meters, exceptionally ~100 m, and elevations around ∼10 m.

5.2.3. Moraine terrain

Moraine terrain is characterized by an undulating surface with diffused irregular features that rise ~10 m from adjacent terrain (Figure 3(b)). It occurs at inner positions, especially nested within the Segunda Angostura drift (i.e. C limit). Sharp moraine ridges are superimposed on this landform (Clapperton, 1989). Punctually, subparallel diffused lineations are visible on its surface, similar to thrusted moraine block recently reported in Lago Viedma (Ponce, González Guillot, Díaz Balocchi, & Martínez, 2019).

5.2.4. Ribbed moraine ridges

The ribbed moraine ridges (Figure 4) are low relief ridges transverse to the inferred glacier flow. They occur as dense groups of ridges characterized by gentle slopes, flat tops and planform that varies from hummocky to anastomosing (Dunlop & Clark, 2006). Previous maps on the region have identified similar features as irregular dissected ridges, avoiding any genetic inference (Darvill et al., 2014; Lovell et al., 2011). The ribbed moraine ridges may reach ~700 m long, ~200 wide and ~10 m high and often appear delimitated by minor lacustrine basin and channel. Well-developed ribbed moraine ridges are located on the Primera Angostura peninsula.

5.2.5. Ribbed moraine terrain

Ribbed moraine terrain (Figure 4) is typically composed of patches of diffused ribbed moraine ridges that cover extensive areas within the ice limits of former ice sheets (Eyles, Boyce, & Barendregt, 1999; Hättestrand & Kleman, 1999). Previous studies on the region have identified this feature as subdued moraine topography (Darvill et al., 2014; Lovell et al., 2011). We differentiated this landform assemblage from moraine terrain based on the presence of diffused flat-topped ridges and their transverse direction relative to the assumed ice-flow (Dunlop & Clark, 2006). The area between Primera and Segunda Angostura is profusely covered by this feature. It occurs on a lower

Table 2. Summary of glacial landforms, identification criteria, uncertainties and previous mapping of the geomorphology of the Magellan ice lobe (adapted from Bendle, Thorndycraft, & Palmer, 2017; Darvill et al., 2014; Lovell et al., 2011).

Landform/ feature	Morphology	Identification criteria	Uncertainties	Interpretation	Previous mapping
Moraine drift	Large linear positive-relief. Undulating topography with distinctive moraine ridges on top.	Elevated above adjacent topography. Coarse grained texture on DEM. Irregular top on aerial and satellite imagery.	Lower sections may appear diffuse when associated with outwash plains. Difficult to distinguish from moraine terrain when both units are closely spaced.	Marks approximate former terminal position of the glacier front.	Caldenius (1932); Meglioli (1992); Clapperton et al. (1995); Benn and Clapperton (2000); Bentley et al. (2005), Darvill et al. (2014)
Moraine ridge	Minor ridges linear to arcuate positive-relief. Sharp crestlines.	Small ridges with dark/light shading on opposing sides in aerial and satellite imagery. Often aligned in the same direction, parallel to main moraine drifts.	Small ridges may be difficult to identify in satellite imagery. Often visible in aerial photos. Moraine ridges can be misidentified with other linear features, such as eskers or paleoshore lines.	Marks approximate temporal ice-front position.	Clapperton et al. (1995); Benn and Clapperton (2000); Bentley et al. (2005); Darvill et al. (2014); Lovell et al. (2011)
Moraine terrain	Patches of subdued irregular topography at similar elevation that moraine drifts. Presence of distinctive sharp moraine ridges.	Areas elevated above adjacent topography. Diffused irregular pattern marked in changes in color and vegetation in aerial and satellite imagery. Medium to coarse grained texture on DEM.	Difficult to classified under a unique criterion due to the profuse irregularity of the feature. Boundaries of moraine terrain are not sharp when associated with moraine drifts. Field-checking is needed for proper identification.	Marks approximate former ice-marginal zone.	Unmapped
Ribbed moraine ridge	Small and flat-topped ridges with subtle topography. Highly irregular plan morphology.	Flat-topped ridges marked by changes in color contrasting adjacent topography in aerial and satellite imagery. Medium to coarse grained texture on DEM	Drainage can sometimes give the illusion of ridges. Delimitation of individual ridges depends almost exclusively on changes in color and vegetation. The general pattern and orientation of the ridges is problematic to observe at the field scale.	Marks approximate former ice-marginal zone. Indicative of former ice- flow direction.	Lovell et al. (2011); Darvill et al. (2014)
Ribbed moraine terrain	Patches of wide and flat-topped ribbed moraine ridges with no obvious orientation. Often delineated by minor channels and lacustrine basins.	Areas of smooth flat-topped ridges with no obvious orientation marked in changes in color and frequent minor lacustrine basins and channels delimitating diffused ridges in aerial and satellite imagery Medium to coarse grained texture on DEM.	When diffused topography is difficult to differentiate from moraine terrain. The organized nature of the feature is only visible on aerial photos and multispectral satellite imagery. The general pattern and orientation of the ridges is problematic to observe at field scale.	Marks approximate former ice-marginal zone.	Unmapped
Kettle topography	Discreet areas of disorganized hills and hollows. Frequent groups of small lakes.	Area with pock-marked topography with marked hollows. Groups of small lakes in aerial and satellite imagery. Coarse grained texture on DEM.	Sometimes difficult to distinguish from esker field and moraine terrain.	Marks approximate former ice-marginal zone or area of stagnant ice.	Clapperton et al. (1995); Benn and Clapperton (2000); Bentley et al. (2005); DeMuro et al. (2015, 2017)
Glacial lineations	Minor linear features aligned to inferred ice- flow.	Linear features with dark/light shading on opposite sides in aerial and satellite imagery. Parallel to the inferred ice-flow. Often appearing in groups. Not associated with breaks on the slope in DEM.	Misclassification of subdued drumlins as lineations. Minor lineations may be difficult to distinguish from irregular topography.	Indicative of former ice- flow direction.	Clapperton (1989); Benn and Clapperton (2000); Bentley et al. (2005); Lovell et al. (2011); Darvill et al. (2014); DeMuro et al. (2017)
Drumlins	Prominent linear hills aligned to inferred ice- flow.	Linear hills with dark/light shading on opposite sides in aerial and satellite imagery. Parallel to the inferred ice-flow. Often appearing in groups. Associated with breaks in the slope in DEM	Subdued drumlins may be difficult to distinguish from lineations or moraine terrain.	Indicative of former ice- flow direction.	Clapperton (1989); Benn and Clapperton (2000); Bentley et al. (2005); Lovell et al. (2011); Darvill et al. (2014); DeMuro et al. (2017)
Drumlinized terrain	Areas dominated by subdued alignment topography. Diffused linear features parallel to inferred ice-flow	Areas of diffused linear hills parallel to the inferred ice-flow. Marked by changes in colors and vegetation in satellite imagery. Subdued breaks in the slope in DEM.	Drumlinized terrain may be difficult to distinguish from moraine terrain.	Indicative of former ice- flow direction.	Clapperton et al. (1995)
Outwash plain	Large approximately flat surface graded from ice-margin features. Presence of distinctive scarps defining a sequence of terraces. Often dissected by channels network.	Areas of homogeneous color imprinted by tracts and channels in aerial and satellite imagery. Fine grained texture with marked linear breaks in the slope delimitating terrace levels in DEM.	Potential misclassification of channels and outwash plains when appear in valleys. Exact limits of outwash are often difficult to delimit when	Indicative of major meltwater drainage pathways	Caldenius (1932); Clapperton et al. (1995); Benn and Clapperton (2000); Bentley et al. (2005); Lovell et al. (2011); Darvill et al.

Outwash scarp	Linear and continuous breaks in the slope of the outwash, delimitating different levels of outwash terraces	Linear features associated with outwash plains and marked by shadowing in aerial and satellite imagery. Sharp breaks in the homogeneous	associated with coastal features. Surface grading only apparent on DEM. Outwash scarps are difficult to separate from meltwater channel scarps.	Marks different stages of outwash construction.	(2014); DeMuro et al. (2015, 2017) Clapperton et al. (1995); Bentley et al. (2005)
Meltwater channel	Deeply incised channel, generally step-sided. Straight to meandering planform. Rarely contain modern drainage routes. Punctual presence of small lacustrine basins.	slope of outwash plains in DEM. Continuous features often associated to outwash plains and terraces and/or running parallel to moraine drifts. Straight to sinuous planform. Margins defined by shadowing in aerial and satellite imagery. Delimitated by sharp changes in the slope and wide flat bottoms in DEM.	Often occupied by streams, so misidentification with modern drainage network is possible.	Delimitates approximate position of the glacier lateral margins. Indicates significant ice fusion.	Clapperton et al. (1995); Benn and Clapperton (2000); Bentley et al. (2005); Lovell et al. (2011); Darvill et al. (2014); DeMuro et al. (2015, 2017)
Esker	Linear to arcuate positive relief ridges or conical mounds mainly composed by beds of sands and gravels. Sharp to rounded crestlines.	Linear to arcuate planform. Dark/light shading on opposing sides in aerial and satellite imagery.	Minor features difficult to identify even in aerial and satellite imagery. Potential confusion with moraine ridges.	Indicative of marginal subglacial drainage configuration	Clapperton (1989); Benn and Clapperton (2000); Bentley et al. (2005); Lovell et al. (2011); Darvill et al. (2014)
Esker field	Areas dominated by esker ridges presenting a highly irregular planform.	Highly irregular planform. Dark/light shading on opposing sides in aerial and satellite imagery. Coarse grained texture on DEM.	Potential confusion with kettle topography. Fieldwork is needed for correct identification.	Marks approximate former ice-marginal zone or area of stagnant ice.	Unmapped
Lacustrine basin	Flat surfaces of light to dark fine-grained sediments. Usually associated to ribbed moraine terrain and present lakes.	Distinctive colors from adjacent terrain, ranging from light to dark coloration in satellite imagery. Normally associated to paleoshore lines either lacustrine or marine. Homogeneous surface texture in DEM's.	Potential misidentification with homogeneous flat surfaces, such as outwash plains and coastal features in DEM.	Indicative of former lake extent.	DeMuro et al. (2015, 2017)
Landslides	Prominent breaks on the slope originating a steeped topography with presence of linear features and small lacustrine basins or masswasting deposits with signs of downslope flow associated to semi-circular scarps in the headwall.	Discreet areas with steeped or depressed topography delimitated by linear scarps. Aligned small lakes and/or transverse ridges to the direction of the slope are frequent in satellite and aerial imagery. Sharply marked by breaks in the slope in DEM.	No significant changes in color in comparison with moraine ridges or moraine terrain. Landslide ridges are easily misidentified as moraine ridges or paleoshore lines. Flowslide deposits are similar to moraine terraine. DEM and fieldwork are needed for proper identification.	Indicative of slope instability.	Unmapped
Coastal features	Sequence of nearly flat terraces delimited by minor scarps and sea cliffs. The lowest terrace level is dominated by sandy beaches and spits.	Areas of homogeneous light colors close to the coastline. Berms are often visible in aerial and satellite imagery. Fine grained texture with subtle linear breaks in the slope delimitating marine terrace levels in DEM.	Difficult to delimitate when associated with outwash plains. Aeolian processes may blur the limits of the features.	Marks areas dominated by marine processes.	Clapperton et al. (1995); Bentley et al. (2005); DeMuro et al. (2015, 2017)
Paleoshoreline	Near-continuous curvilinear feature. Minor break in slope at water-side, flat surface grading out from the water body.	Closely associated to local water bodies. Normally parallel to present coastline. Only visible in aerial and satellite imagery.	Difficult to see in DEM's. Sometimes similar to minor moraine ridges.	Marks former elevation of local water plains, either sea or lake levels.	Bentley et al. (2005); Lovell et al. (2011); Darvill et al. (2014)

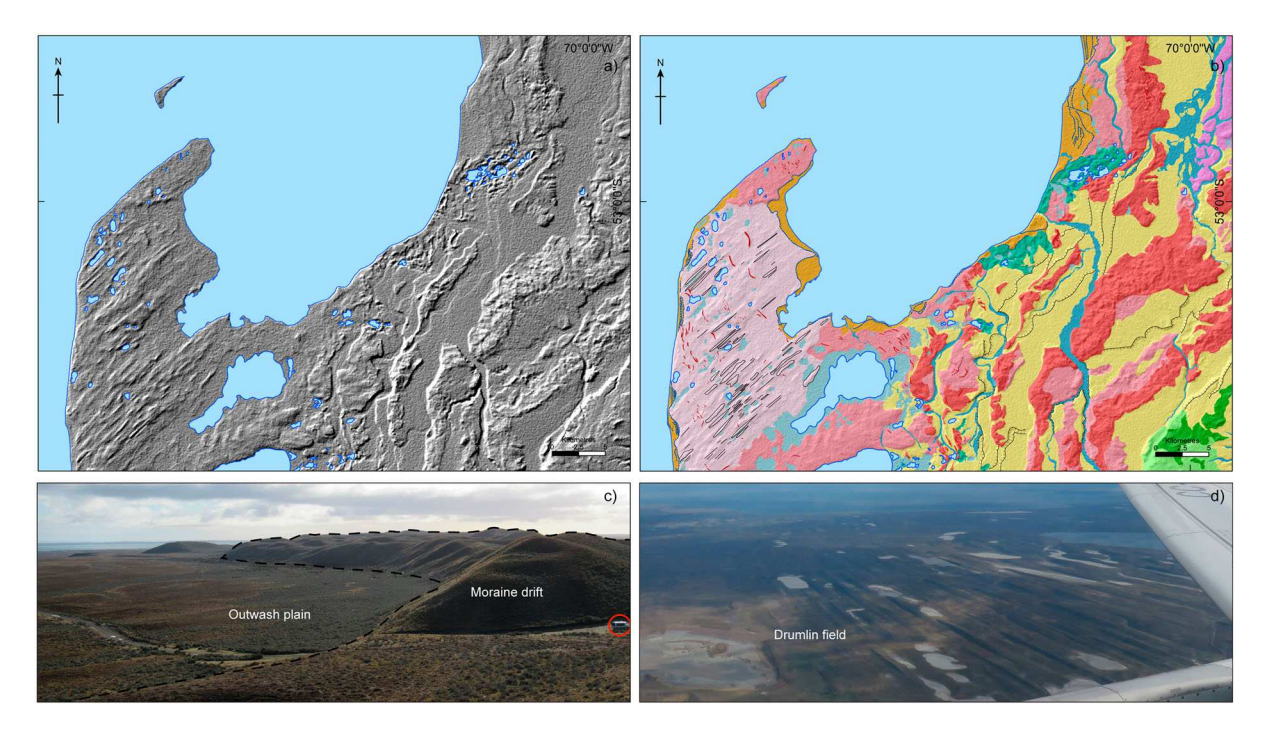


Figure 3. (a) Hillshade representation from ALOS PALSAR digital elevation model showing different terrain textures in the southern area of Juan Mazía Península. Predominant textures were interpreted as moraine drift (coarse texture) and outwash plain (smooth texture). (b) Geomorphic map showing ILGM glacial drifts (dark pink), ILGM moraine terrain (light pink), pre-ILGM glacial drifts (dark green), pre-ILGM moraine terrain (light green), outwash plains (yellow), outwash scarps (black dashed line), major meltwater channels (dotted light blue), kettle topography (turquoise), drumlins (black polygon), lineations (black line). (c) Detail of the major glacial drifts and outwash plains (vehicle for scale). (d) Aerial view of the drumlin field north of Punta Arenas.

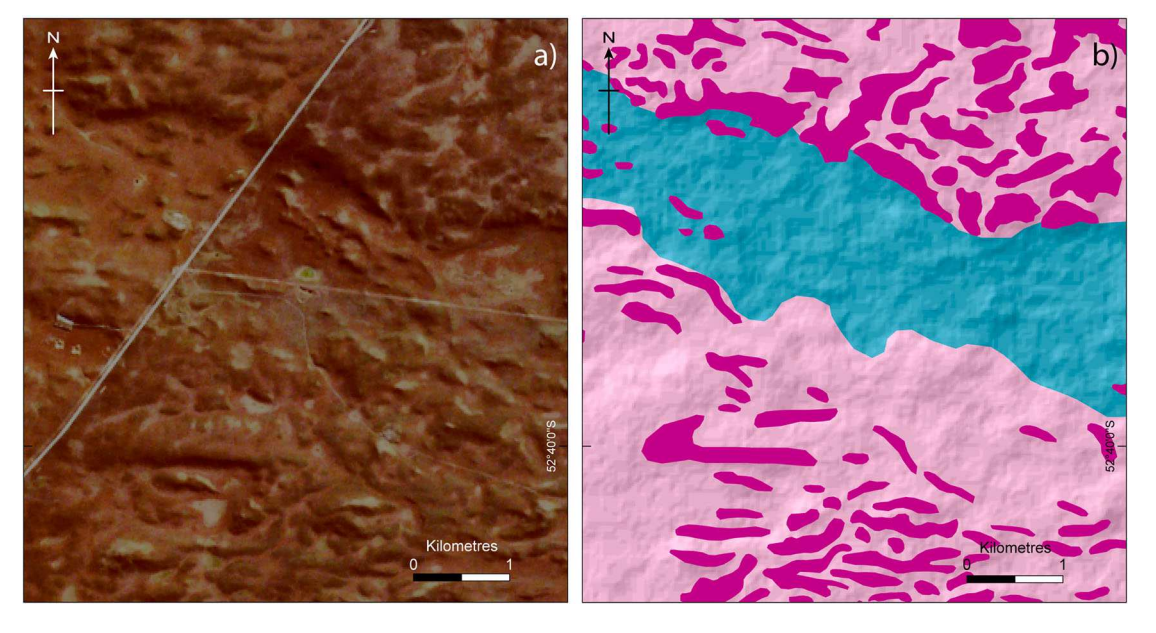


Figure 4. (a) Satellite image (Sentinel 2) showing the ribbed moraine terrain near Primera Angostura. (b) Geomorphic map showing ribbed moraine terrain (purple), ribbed moraine ridges (dark purple) and melwater channel (blue).

topographical position than moraine drifts, at elevations ranging from ~60 to ~10 m.a.s.l. Small lacustrine basins and minor channel are frequently associated to this landform.

5.2.6. Kettle topography

Kettle topography (Figure 3(b)) is defined by groups of semi-circular hollows flanked by rim ridges, formed by

the disappearance of stagnant pieces of ice separated from the main ice lobe (Supplementary map). They are closely associated with proximal slopes of the youngest moraine drifts, mainly in Gente Grande Bay area. The geometry of the kettle pits is variable. However, most of them have diameters ranging between tens to hundreds of meters and maximum depths of \sim 20 m.

5.3. Subglacial features

5.3.1. Glacial lineations

Glacial lineations consist of linear landforms with a strong common orientation parallel to inferred iceflow (Figure 3; Spagnolo et al., 2014). Many of these landforms were previously mapped in the Strait of Magellan area by Darvill et al. (2014) and Lovell et al. (2011), who used them to reconstruct former ice lobe dynamics (Darvill et al., 2016; Lovell, Stokes, Bentley, & Benn, 2012).

We found glacial lineations mostly around Gente Grande Peninsula and north of the Strait of Magellan. In both areas, they are associated with other ice floworiented landforms such as drumlins or ribbed moraine ridges. Glacial lineations rarely are greater than 1 km in length and a few meters high.

5.3.2. Drumlins and drumlinized terrain

Drumlins are large-scale, asymetrical glacial lineations aligned parallel to ice flow direction and formed beneath ice sheets (Figure 3; Smith et al., 2007). They were first described in the region by Clapperton (1989) and subsequently mapped by Darvill et al. (2014) and Lovell et al. (2011).

The largest drumlin fields in the study area are located on Gente Grande Peninsula and northern Strait of Magellan. The orientation of the drumlins indicates a SW-NE and S-NW ice flow direction, respectively. In these areas, single drumlins reach >1 km in length and tens of meters in height. Elongated lacustrine basins are common between the drumlinized landforms. In addition, this area contains individual moraine ridges overlying the drumlins.

Drumlinized terrain is defined as an area with a high concentration of poorly-defined drumlins. Previous studies have identified ice-thrusted glacial sediments forming drumlin-like features covering extensive areas in the north of the Strait of Magellan and classified them as cupola hills (Benn & Clapperton, 2000).

5.4. Glaciofluvial features

5.4.1. Outwash plains

Outwash plains (Figure 3) are the major glaciofluvial landform found in the Strait of Magellan area. They are gently sloping surfaces built on glaciofluvial sands and gravels. They are extensive on the north-eastern sector of the study area, especially in both the Primera Angostura and Juan Mazía peninsulas. Outwash plains are intensely scoured by intricate channel networks, most of which are inactive today. Associated with moraine drift slopes are different terrace levels, which suggest multiple stages of outwash construction.

5.4.2. Meltwater channels

Meltwater channels are another major glaciofluvial landform in the area (Supplementary map). They appear closely associated with outwash plains, where they imprint a complex fluvial network, as well as moraine drifts, where they commonly run parallel or cross cut them (Bentley et al., 2005). The plan morphology of the meltwater channels ranges from straight to meandering. Their lengths reach up to ~100 km and their widths range from tens to hundreds of meters. The presence of terraces on their slopes is common. These channels often contain small lake basins.

5.4.3. Eskers and esker field

Eskers are sinuous ridges built on beds of sand and gravels and occasionally till (Figure 5) in subglacial







Figure 5. (a) Satellite image (ESRI imagery) showing esker terrain and mounds located south of Porvernir. (b) Detail of a sinuous esker ridge near Porvenir (person for scale). (c) Exposure through an esker ridge, which is mainly composed by alternate beds of sand and gravels (field book for scale).

meltwater channels (Storrar, Stokes, & Evans, 2014). These features were first identified by Clapperton (1989) and Lovell et al. (2011) in the north inland of the Strait of Magellan. Eskers can reach hundreds of meters in length and rarely more than ~10 meters in height. Unlike other linear features, they range from conical mounds to single or interconnected highly sinuous ridges in planform.

Near Porvenir, these features form extensive fields of interconnected sandy to gravelly ridges, producing a highly irregular pattern of elongated hills and hollows. We interpret this landform assemblage as an ice stagnation topography (Ponce et al., 2019; Schomacker, 2008).

5.5. Other features

5.5.1. Lacustrine basins

Flat surfaces composed of light to dark sediments closely related to existing lakes, paleoshore lines, ribbed moraine terrain, drumlinized terrain or inactive channels. They can be periodically flooded (Supplementary map).

5.5.2. Landslides

We identified what we infer to be rotational landslides and flowslides near to Altos del Boquerón and Cordón Baquedano, respectively. Rotational landslides (Figure 6) consist of a stepped sequence of well-defined linear scarps separated by narrow flat surfaces, occupied by small lakes and transverse ridges. Previous works depicted these landforms as former shorelines and moraine ridges (Darvill et al., 2014). However, based on direct observations, we conclude that these areas are dominated by landslide deposits and scarps. Moreover, recent works have also reported large rotational landslides associated with glacial landscapes in central Patagonia (Pánek, Korup, Lenart, Hradecký, & Břežný, 2018). Flowslides are characterized by the presence of a semi-circular scarps on the headwalls of mass-wasting deposits with signs of downslope flow, such as transverse crevasses and ridges (Figure 6).

5.5.3. Coastal features and paleoshore lines

Groups of coastal features and paleoshorelines are present across the study area (Figure 3). Previous studies have identified a sequence of at least four marine terraces in Juan Mazía Peninsula and Gente Grande Bay (DeMuro et al., 2015; 2017). These features appear as a succession of scarps with maximum heights reaching ~20 meters. These sea cliffs are mostly built on glacial, glaciofluvial and aeolian deposits. The lowest level of marine terraces is dominated by sandy beaches and other depositional landforms, such as spits (e.g. near San Gregorio Cape, Primera Angostura Peninsula).

Paleoshore lines are linear and continuous landforms which generally run parallel to modern sea or lake coastlines. They exhibit no positive relief and small scarps facing present water-bodies. These features indicate the former level of lakes and ocean.

6. Final remarks and conclusions

A new detailed map of the landforms created by the Magellan ice lobe provides insight in the structure of the regional glacial fluctuations and sets the spatial frame for establishing the timing of past ice-sheet activity. Glacial and glaciofluvial features dominate

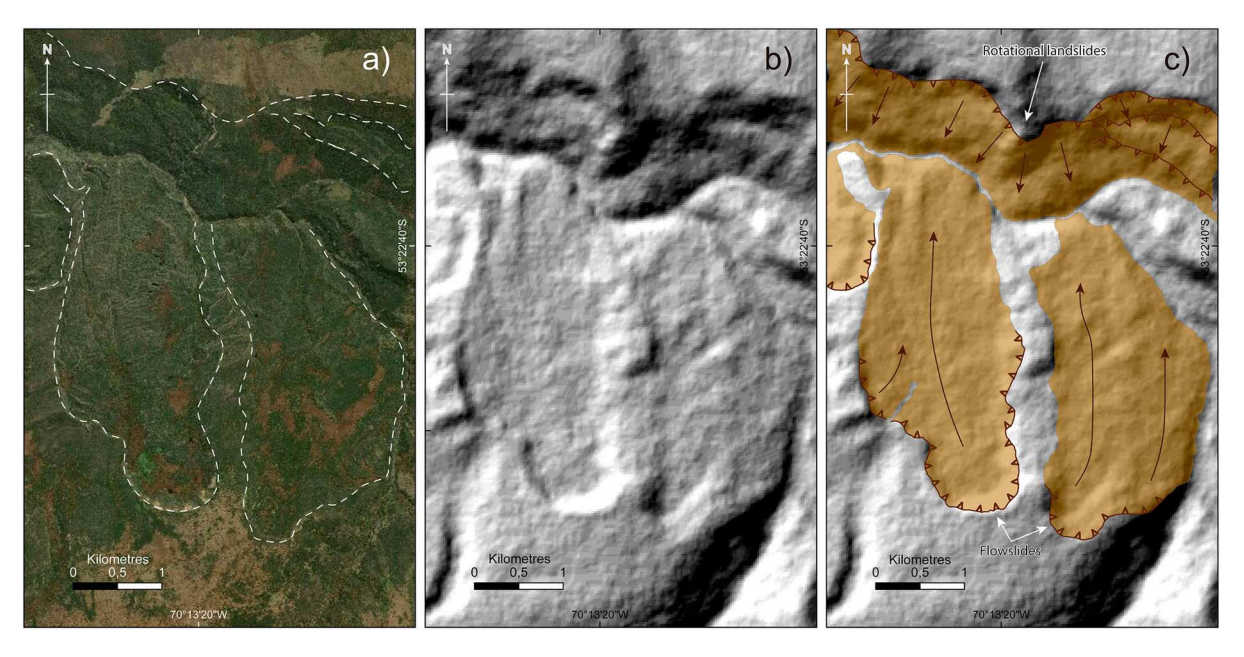


Figure 6. (a) Satellite image (ESRI imagery) showing landslides in Cordón Baquedano area. Contour of major landslide deposits are presented in white dashed line. (b) ALOS PALSAR digital terrain model of the landslides in Cordón Baquedano area. (c) Geomorphic map of the Cordón Baquedano area illustrating the extent of landslide deposits and main landslide crowns.

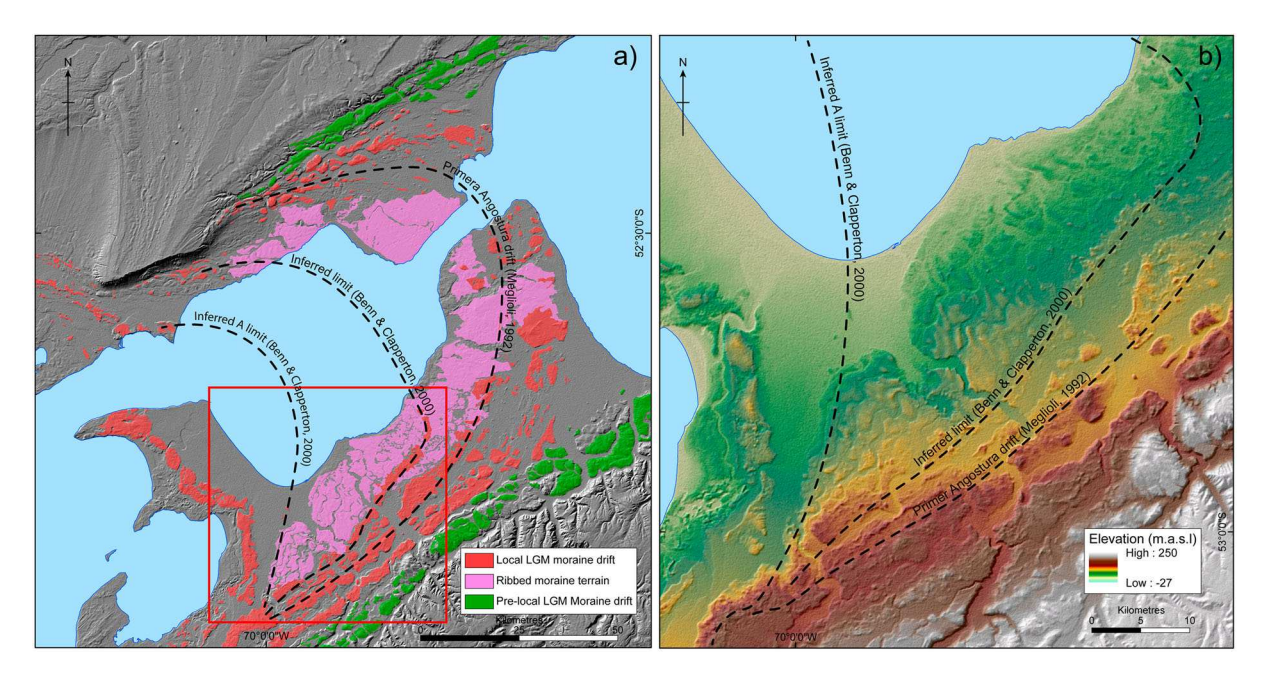


Figure 7. (a) Map of the major moraine drifts in the area between Juan Mazia and Primera Angostura peninsulas. The inferred limits proposed by Benn and Clapperton (2000) and Meglioli (1992) are shown as a dashed black line. (b) ALOS PALSAR digital elevation model of the southern Juan Mazía Peninsula area.

the landscape, especially moraine drifts and meltwater channels imprinted over extensive outwash plains.

We map at least five glacial limits and extend in detail the spatial knowledge of surface features eastward towards the Atlantic Ocean (Figure 2(a)). The innermost moraine complexes (red on map) correspond to the C, B (i.e. Juan Mazía drift) and A limits (Figure 2(b)) previously defined by Clapperton et al. (1995). Geomorphic evidence leads us to infer that the A limit splits into, at least, two branches, and possibly three (Figure 7(a)). The inner moraine branch, represented by minor positive relief features appearing over Juan Mazía outwash, would correspond to the A limit as originally defined by Benn and Clapperton (2000; Figure 7(b)). The intermediate moraine branch runs to the northeast at ~60 m.a.s.l. and turns towards San Felipe Bay (Figure 7(b)). The outer moraine branch continues between ~120 and ~80 m.a.s.l. to the Primera Angostura Peninsula, where it adopts a frontal position across the Strait of Magellan (Figure 7(a)).

Based on geomorphic evidence, we consider the A limit to be a composite set of landforms created over successive advances of the Magellan ice lobe to lateral positions south and east of Juan Mazía Peninsula. Therefore, Meglioli's Primera Angostura drift likely corresponds to an early frontal position of Clapperton's A limit, and the inner limits depicted by Benn & Clapperton represent minor advances or standstills of the Magellan ice lobe before the construction of the B limit.

In addition, we recalculate previously-published cosmogenic ages (Figure 8) on boulders from the Primera Angostura/A limit with updated systematics (e.g. Kaplan et al., 2011); these are 36.6 ± 4.0 , $26.8 \pm$

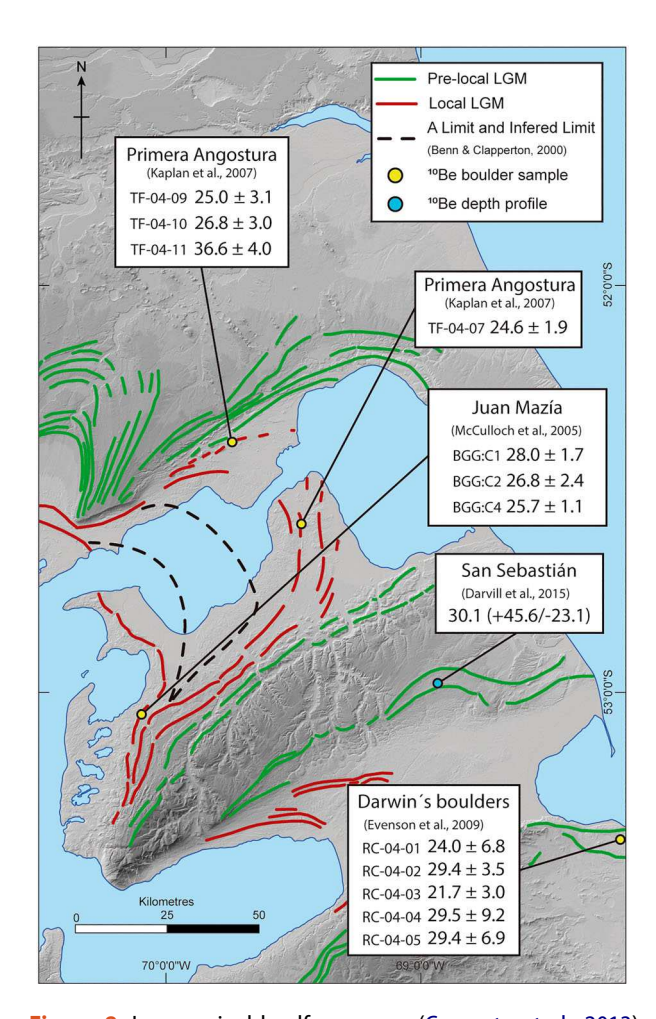


Figure 8. Ice-marginal landforms map (Coronato et al., 2013) showing recalculated ¹⁰Be ages on moraine boulders on Primera Angostura and Juan Mazía (Kaplan et al., 2007; McCulloch et al., 2005) and cosmogenic ages from erratic boulders (Evenson et al., 2009) and vertical transect in outwash gravels near Bahía Inútil (Darvill et al., 2015). We excluded ages that authors considered outliers.

3.0, 25.0 ± 3.1 and 24.6 ± 1.9 ka (Kaplan et al., 2007). Taken at face value, these ¹⁰Be ages constrain the formation of the Primera Angostura/A limit between ~24 and ~36 ka, supporting glaciations also during early MIS 2 and perhaps in late MIS 3. In addition, cosmogenic ages from erratic boulders and vertical profiles in outwash gravels associated with the morphostrategraphically older Punta Delgada drift in Bahía Inútil area yielded ages of 24.0 ± 6.8 , 29.4 ± 3.5 , 21.7 ± 3.0 , 29.5 ± 9.2 and 29.4 ± 6.9 ka (Evenson et al., 2009) and ~30.1 ka (Darvill et al., 2015), respectively. Thus, we infer that (i) the Primera Angostura drift (outer A limit) corresponds to a lLGM limit of the Magellan lobe, in contrast with previous studies, which placed its maximum extent at Juan Mazía (B limit) during this time (Clapperton et al., 1995; Kaplan et al., 2007, 2008; McCulloch et al., 2005); (ii) the Magellan lLGM predates the gLGM as also concluded by Darvill et al. (2016).

Beyond the Primera Angostura/A limit we mapped at least one older drift, possibly two (green on supplementary map). These glacial units correspond to a flat-topped lateral moraine, heavily incised by fluvial drainage, which might be correlative to Punta Delgada and Cabo Vírgenes drifts, respectively (Meglioli, 1992). Considering the large uncertainties of the dating constraints of Primera Angostura/A limit (Darvill et al., 2015; Kaplan et al., 2007) and the geomorphic characteristics of these external drifts (Bentley et al., 2005), they could have been deposited during late MIS 3 and more likely prior.

If our interpretation is correct, the Magellan ice lobe would have reached a position ~65 km further east during the last glaciation than previously inferred. These findings will provide a new glacial boundary condition for numerical ice-sheet modeling of the Magellan ice lobe, setting up a new context for future paleoclimatic geomorphic-based reconstructions.

Software

Spatial information analysis was carried out by using ArcGIS 10.3 software. Hillshade extraction from the digital elevation model was performed with Surfer 12. World image in the inset map was compose in MATLAB 2015. Final map production was completed with Adobe Illustrator CC 2017.

Acknowledgements

We are very grateful to José Araos, Juan Carlos Aravena, Gonzalo Amigo, Alberto Rendoll and Lauren Robinson for field assistance. We also like to thank John Clague, Cristopher Darvill and Chris Orton for contributing to significantly improve the manuscript. This is LDEO contribution #8383.

Disclosure statement

No potential conflict of interest was reported by the author(s).

Funding

This research was supported by National Ph.D. Fellowship CONICYT #21161417 (Soteres), FONDECYT #1160488 (Sagredo), ANID Millennium Science Initiative/"Millennium Nucleus Paleoclimate" (Soteres & Sagredo) and National Sciences Foundation NSF-BCS 1263474 (Kaplan) and a Fulbright Commission Visiting Scholar Grant (Kaplan).

ORCID

Rodrigo L. Soteres http://orcid.org/0000-0003-3647-5342

References

Bendle, J. M., Thorndycraft, V. R., & Palmer, A. P. (2017). The glacial geomorphology of the Lago Buenos Aires and Lago Pueyrredón ice lobes of central Patagonia. Journal of Maps, 13(2), 654-673. http://doi.org/10.1080/ 17445647.2017.1351908

Benn, D. I., & Clapperton, C. M. (2000). Pleistocene glacitectonic landforms and sediments around central Magellan Strait, southernmost Chile: Evidence for fast outlet glaciers with cold-based margins. Quaternary Science Reviews, 19, 591-612.

Bentley, M. J., Sugden, D. E., Hulton, N. R. J., & McCulloch, R. D. (2005). The landforms and pattern of deglaciation in the Strait of Magellan and Bahia Inutil, southernmost South America. Geografiska Annaler, Series A: Physical Geography, 87(2), 313-333. doi:10.1111/j.0435-3676. 2005.00261.x

Blomdin, R., Murray, A., Thomsen, K. J., Buylaert, J. P., Sohbati, R., Jansson, K. N., & Alexanderson, H. (2012). Timing of the deglaciation in southern Patagonia: Testing the applicability of K-Feldspar IRSL. Quaternary Geochronology, 10, 264-272. doi:10.1016/j.quageo.2012. 02.019

Bujalesky, G., Coronato, A., & Isla, F. (2001). Ambientes glaciofluviales y litorales cuaternarios de la región del río Chico, Tierra del Fuego, Argentina. Revista de la Asociación Geológica Argentina, 56(1), 73–90.

Butorovic, N. (2016). Resumen meteorológico año 2015. Estación "Jorge Schyte" (53 08 S; 70 53 O; 6 msnm). Anales de Instituto de La Patagonia, 44(1), 1-10.

Caldenius, C. C. (1932). Las glaciaciones cuaternarias en la Patagonia y Tierra del Fuego. Geografiska Annaler, Series A: Physical Geography, 14, 1-164.

Chandler, B., Lovell, H., Boston, C. M., Chandler, B. M. P., Lovell, H., Boston, C. M., ... Otto, J. (2018). Glacial geomorphological mapping: A review of approaches and frameworks for best practice. Earth-Science Reviews, 185, 806-846. doi:10.1016/j.earscirev.2018.07.015

Clague, J. J., Barendregt, R. W., Menounos, B., Roberts, N. J., Rabassa, J., Martínez, O., Ercolano, B., Corbella, H., & Hemming, S. D. (2020). Pliocene and early Pleistocene glaciation and landscape evolution on the Patagonian Steppe, Santa Cruz province, Argentina. Quaternary Science Reviews, 227, 105992. https://doi.org/10.1016/j. quascirev.2019.105992

- Clapperton, C. M. (1989). Asymmetrical drumlins in Patagonia, Chile. Sedimentary Geology, 62(2-4), 387-398. doi:10.1016/0037-0738(89)90127-9
- Clapperton, C. M., Sugden, D. E., Kaufman, D. S., & McCulloch, R. D. (1995). The last glaciation in central Magellan Strait, southernmost Chile. Quaternary Research, 44(2), 133-148. doi:10.1006/qres.1995.1058
- Coronato, A., Ercolano, B., Corbella, H., & Tiberi, P. (2013). Glacial, fluvial and volcanic landscape evolution in the Laguna Potrok Aike area, Southern Patagonia, Argentina. Quaternary Science Reviews, 71, 13-26. http://doi.org/10.1016/j.quascirev.2012.06.019
- Coronato, A., Meglioli, A., & Rabassa, J. (2004). Glaciations in the magellan straits and tierra del fuego, southernmost South America. In J. Ehlers & P. L. Gibbard (Eds.), Developments in quaternary sciences, Vol. 2 (C) (pp. 45-48). Amsterdam: Elsevier.
- Darvill, C. M., Bentley, M. J., Stokes, C. R., Hein, A. S., & Rodés, Á. (2015). Extensive MIS 3 glaciation in southernmost Patagonia revealed by cosmogenic nuclide dating of outwash sediments. Earth and Planetary Science Letters, 429, 157–169. doi:10.1016/j.epsl.2015.07.030
- Darvill, C. M., Stokes, C. R., Bentley, M. J., Evans, D. J. A., & Lovell, H. (2016). Dynamics of former ice lobes of the southernmost Patagonian Ice Sheet based on a glacial landsystems approach. doi:10.1002/jqs.2890
- Darvill, C. M., Stokes, C. R., Bentley, M. J., & Lovell, H. (2014). A glacial geomorphological map of the southernmost ice lobes of Patagonia: The Bahía Inútil - San Sebastián, Magellan, Otway, Skyring and Río Gallegos lobes. Journal of Maps, 10 (3), 500-520. doi:10.1080/17445647.2014.890134
- DeMuro, S., Brambati, A., Tecchiato, S., Porta, M., & Ibba, A. (2017). Geomorphology of marine and transitional terraces and raised shorelines between Punta Paulo and Porvenir, Tierra del Fuego, Strait of Magellan - Chile. Journal of Maps, 13(2), 311-321. doi:10.1080/17445647. 2017.1295406
- DeMuro, S., Di Grande, A., Brambati, A., & Ibba, A. (2015). Geomorphology map of the marine and transitional terraces and raised shorelines of the Península Juan Mazía, Tierra del Fuego. Strait of Magellan - Chile. Journal of Maps, 11(5), 698-710. doi:10.1080/17445647.2014.970592
- Denton, G. H., Lowell, T. V., Heusser, C. J., Schlüchter, B. G., Andersen, B. G., Heusser, L. E., Moreno, P. I., & Marchant, D. R. (1999a). Geomorphology, stratigraphy, and radiocarbon chronology of Llanquihue drift in the area of the Southern Lake District, Seno Reloncaví, and Isla Grande de Chiloé. Geografiska Annaler Series A-Physical Geography, 81(2), 167-229.
- Denton, G. H., Lowell, T. V., Heusser, C. J., Schlüchter, B. G., Andersen, B. G., Heusser, L. E., Moreno, P. I., & Marchant, D. R. (1999b). Interhemispheric linkage of paleoclimate during the last glaciation. Geografiska Annaler Series A-Physical Geography, 81(2), 107-153.
- Douglass, D., Singer, B., Kaplan, M., Mickelson, D. M., & Caffee, M. W. (2006). Cosmogenic nuclide surface exposure dating of boulders on last-glacial and late-glacial moraines, Lago Buenos Aires, Argentina: Interpretive strategies and paleoclimate implications. Quaternary Geochronology, 1(1), 43-58.
- Dunlop, P., & Clark, C. D. (2006). The morphological characteristics of ribbed moraine. Quaternary Science Reviews, 25, 1668-1691. doi:10.1016/j.quascirev.2006.01.002
- Evenson, E., Burkhart, P., Gosse, J., & Baker, G. (2009). Enigmatic boulder trains, supraglacial rock avalanches, and the origin of "Darwin's boulders," Tierra del Fuego. GSA Today, 19(12), 4-10.

- Eyles, N., Boyce, J. I., & Barendregt, R. W. (1999). Hummocky moraine: Sedimentary record of stagnant Laurentide Ice Sheet lobes resting on soft beds. Sedimentary Geology, 123(3-4), 163-174. doi:10.1016/ S0037-0738(98)00129-8
- Garreaud, R. D., Vuille, M., Compagnucci, R., & Marengo, J. (2009).Present-day South American climate. Palaeogeography, Palaeoclimatology, Palaeoecology, 281 (3-4), 180-195. doi:10.1016/j.palaeo.2007.10.032
- Garreaud, R., Lopez, P., Minvielle, M., & Rojas, M. (2013). Large-scale control on the Patagonian climate. Journal of Climate, 26(1), 215–230. doi:10.1175/JCLI-D-12-00001.1
- Glasser, N. F., & Jansson, K. N. (2008). The glacial map of Southern South America. Journal of Maps, 4(1), 175-196. doi:10.4113/jom.2008.1020
- Glasser, N. F., Jansson, K. N., Harrison, S., & Kleman, J. (2008). The glacial geomorphology and Pleistocene history of South America between 38°S and 56°S. Quaternary Science Reviews, 27, 365–390. doi:10.1016/j. quascirev.2007.11.011
- Hall, B. L., Porter, C. T., Denton, G. H., Lowell, T. V., & Bromley, G. R. M. (2013). Extensive recession of Cordillera Darwin glaciers in southernmost South America during Heinrich Stadial 1. Quaternary Science Reviews, 62, 49-55. doi:10.1016/j.quascirev.2012.11.026
- Hättestrand, C., & Kleman, J. (1999). Ribbed moraine formation. Quaternary Science Reviews, 18(1), 43-61. doi:10.1016/S0277-3791(97)00094-2
- Hein, A. S., Cogez, A., Darvill, C. M., Mendelova, M., Kaplan, M. R., Herman, F., Dunai, T. J., Norton, K., Xu, S., Christl, M., & Rodés, Á. (2017). Regional mid-Pleistocene glaciation in central Patagonia. Quaternary Science Reviews, 164, 77-94. https://doi.org/10.1016/j.quascirev.2017.03.
- Hein, A. S., Hulton, N. R. J., Dunai, T. J., Schnabel, C., Kaplan, M. R., Naylor, M., & Xu, S. (2009). Middle Pleistocene glaciation in Patagonia dated by cosmogenic-nuclide measurements on outwash gravels. Earth and Planetary Science Letters, 286(1), 184-197. doi:10. 1016/j.epsl.2009.06.026
- Hein, A. S., Hulton, N. R. J., Dunai, T. J., Sugden, D. E., Kaplan, M. R., & Xu, S. (2010). The chronology of the Last Glacial Maximum and deglacial events in central Argentine Patagonia. Quaternary Science Reviews, 29(9-10), 1212-1227.
- Kaplan, M. R., Ackert, R. P., Singer, B. S., Douglass, D. C., & Kurz, M. D. (2004). Cosmogenic nuclide chronology of millennial-scale glacial advances during O-isotope stage 2 in Patagonia. Geological Society of America Bulletin, 116(3), 308-321. doi:10.1130/B25178.1
- Kaplan, M. R., Coronato, A., Hulton, N. R. J., Rabassa, J. O., Kubik, P. W., & Freeman, S. P. H. T. (2007). Cosmogenic nuclide measurements in southernmost America and implications for landscape change. Geomorphology, 87(4), 284-301. doi:10.1016/j.geomorph.
- Kaplan, M. R., Douglass, D. C., Singer, B. S., Ackert, R. P., & Caffee, M. W. (2005). Cosmogenic nuclide chronology of pre-Last Glacial Maximum moraines at Lago Buenos Aires, 46°S, Argentina. Quaternary Research, 63(3), 301-315. doi:10.1016/j.yqres.2004.12.003
- Kaplan, M. R., Fogwill, C. J., Sugden, D. E., Hulton, N. R. J., Kubik, P. W., & Freeman, S. P. H. T. (2008). Southern Patagonian glacial chronology for the Last Glacial period and implications for Southern Ocean climate. Quaternary Science Reviews, 27(3-4), 284-294. doi:10.1016/j. quascirev.2007.09.013



- Kaplan, M. R., Strelin, J. A., Schaefer, J. M., Denton, G. H., Finkel, R. C., Schwartz, R., Putnam, A. E., Vandergoes, M. J., Goehring, B. M., & Travis, S. G. (2011). In-situ cosmogenic ¹⁰Be production rate at Lago Argentino, Patagonia: Implications for late-glacial climate chronology. Earth and Planetary Science Letters, 309(1-2), 21-32. https://doi.org/10.1016/j.epsl.2011.06.018
- Lovell, H., Stokes, C. R., & Bentley, M. J. (2011). A glacial geomorphological map of the Seno Skyring-Seno Otway-Strait of Magellan region, southernmost Patagonia. Journal of Maps, 7(1), 318-339. doi:10.4113/ jom.2011.1156
- Lovell, H., Stokes, C. R., Bentley, M. J., & Benn, D. I. (2012). Evidence for rapid ice flow and proglacial lake evolution around the central Strait of Magellan region, southernmost Patagonia. Journal of Quaternary Science, 27(6), 625-638. doi:10.1002/jqs.2555
- Lowell, T. V., Heusser, C. J., Andersen, B. G., Moreno, P. I., Hauser, A., Heusser, L. E., Schluchter, C., Marchant, D. R., & Denton, G. H. (1995). Interhemispheric correlation of late Pleistocene glacial events. Science, 269(5230), 1541-1549. https://doi.org/10.1126/science.269.5230.1541
- Mackintosh, A. N., Anderson, B. M., & Pierrehumbert, R. T. (2017). Reconstructing climate from glaciers. Annual Review of Earth and Planetary Sciences, 45, 649-680. doi:10.1146/annurev-earth-063016-020643
- McCulloch, R., Fogwill, C., Sugden, D., Bentley, M., & Kubik, P. (2005). Chronology of the last glaciation in central Strait of Magellan and Bahía Inútil, southernmost South America. Annaler: Series A, 87(2), 289-312.
- Meglioli, A. (1992). Glacial geology of Southernmost Patagonia, Strait of Magellan and Northern Tierra del Fuego. Ph.D. thesis, Lehigh University, Bethlehem, PA.
- Mercer, J. H. (1976). Glacial history of southernmost South America. Quaternary Research, 6(2), 125-166. doi:10. 1016/0033-5894(76)90047-8
- Nordenskjöld, O. (1899). Geologie, geographie und anthropologie. Scwedischen Expedition nach den Magellansländern, 1895-1897. Stockholm: Norstedt & Söner.
- Pánek, T., Korup, O., Lenart, J., Hradecký, J., & Břežný, M. (2018). Giant landslides in the foreland of the Patagonian Ice Sheet. Quaternary Science Reviews, 194, 39-54. doi:10.1016/j.quascirev.2018.06.028
- Ponce, J. F., González Guillot, M., Díaz Balocchi, L., & Martínez, O. (2019). Geomorphological evidences of paleosurge activity in Lake Viedma Lobe, Patagonia, Argentina. Geomorphology, 327, 511-522. doi:10.1016/j. geomorph.2018.11.023

- Porter, S. C. (1990). Character and ages of Pleistocene drifts in a transect across the Strait of Magellan. Quaternary of South America and Antarctic Peninsula, 7, 35-50.
- Rabassa, J., & Coronato, A. (2009). Glaciations in Patagonia and Tierra del Fuego during the Ensenadan stage/age Pleistocene-earliest middle Pleistocene). Quaternary International, 210(1-2), 18-36. doi:10.1016/ j.quaint.2009.06.019
- Rabassa, J., Coronato, A., Bujalesky, G., Salemme, M., Roig, C., Meglioli, A., Heusser, C., Gordillo, S., Roig, F., Borromei, A., & Quattrocchio, M. (2000). Quaternary of Tierra del Fuego, southernmost South America: An updated review. Quaternary International, 60-71, 217-
- Schomacker, A. (2008). What controls dead-ice melting under different climate conditions? A discussion. Earth-Science Reviews, 90, 103-113. doi:10.1016/j.earscirev. 2008.08.003
- SERNAGEOMIN. (2003). Mapa geológico de Chile: versión digital. Servicio Nacional de Geología y Minería, Publicación Geológica Digital, 4, CD-ROM, versión 1.0.
- Singer, B., Ackert, R., & Guillou, H. (2004). 40Ar/39Ar and K-Ar chronology of Pleistocene glaciations in Patagonia. Geological Society of America Bulletin, 116(3/ 4), 434-450.
- Smith, A. M., Murray, T., Nicholls, K. W., Makinson, K., Adalgeirsdóttir, G., Behar, A. E., & Vaughan, D. G. (2007). Rapid erosion, drumlin formation, and changing hydrology beneath an Antarctic ice stream. Geology, 35 (2), 127-130. doi:10.1130/G23036A.1
- Spagnolo, M., Clark, C. D., Ely, J. C., Stokes, C. R., Anderson, J. B., Andreassen, K., Graham, A. G. C. & King, E. C. (2014). Size, shape and spatial arrangement of megascale glacial lineations from a large and diverse dataset. Earth Surface Processes and Landforms, 39(11), 1432-1448. https://doi.org/10.1002/esp.3532
- Storrar, R. D., Stokes, C. R., & Evans, D. J. A. (2014). Morphometry and pattern of a large sample (>20,000) of Canadian eskers and implications for subglacial drainage beneath ice sheets. Quaternary Science Reviews, 105, 1-25. doi:10.1016/j.quascirev.2014.09.013
- Sugden, D. E., Bentley, M. J., Fogwill, C. J., Hulton, N. R. J., McCulloch, R. D., & Purves, R. S. (2005). Late-glacial glacier events in southernmost South America: A blend of 'northern' and 'southern' hemispheric climatic signals? Geografiska Annaler: Series A, Physical Geography, 87(2), 273-288. doi:10.1111/j.0435-3676. 2005.00259.x